Stepwise changes in the murine salivary gland immune response during virally-induced ectopic lymphoid structure formation

R. Coleby, D. Lucchesi, E. Pontarini, C. Pitzalis, M. Bombardieri

Centre for Experimental Medicine and Rheumatology, William Harvey Research Institute, Queen Mary University of London, London, UK.

*Rachel Coleby, MSc**
*Davide Lucchesi, PhD**
*Elena Pontarini, PhD**
Costantino Pitzalis, FRCP, MD, PhD
Michele Bombardieri, FRCP, MD, PhD

**These authors share first authorship.*

Please address correspondence to:
Michele Bombardieri,
Experimental Medicine and Rheumatology,
William Harvey Research Institute,
Queen Mary University of London,
SE1 9RT London, UK.
E-mail: m.bombardieri@qmul.ac.uk

Received on June 11, 2021; accepted in revised form on August 30, 2021.

Clin Exp Rheumatol 2021; 39 (Suppl. 133): S39-S48.

Key words: Sjögren's syndrome, ectopic lymphoid structures, autoimmune diseases, immune response

Competing interests: none declared.

ABSTRACT

Objective. *Sjögren's syndrome (SS) is a chronic autoimmune disease characterised by lymphocytic infiltration into the salivary glands (SG) and, in a subset of patients, formation of ectopic lymphoid structures (ELS) in the glands. However, the mechanisms of how ELS form ectopically are not fully elucidated. Here we used a viral inducible murine model of ELS formation in the SG to elucidate the key immunological steps regulating the formation of ELS in the SG.*

Methods. *We have utilised an inducible murine model of sialadenitis whereby retrograde cannulation of the submandibular SG with a replication-deficient adenovirus 5 leads to the formation of ELS. Flow cytometry, immunofluorescence and gene expression was performed on the SGs at regular time points after cannulation to follow the organisation of ELS.*

Results. *Innate immune cells (neutrophils, eosinophils and monocytes) rapidly infiltrated the SG by 3 days post cannulation (dpc) whereby monocytes started to differentiate into resident macrophages. Myeloid dendritic cells accumulated inside leukocytic aggregates whereas macrophages were excluded from the developing ELS. Meanwhile, CD11b+ cells upregulated* Il18, Cxcl13, Ltb, April *and other lymphoid genes stimulating the influx of T cells by 12 days and B cells shortly after. Infiltration of T-follicular helper (Tfh) cells correlated with an increase in GL7+ germinal centre B cells, which peaked at 19 dpc.*

Conclusions. *Immune cell infiltration in virally-infected murine SG follows a highly reproducible step-wise process whereby early innate immune cells reshape the SG myeloid compartment leading to upregulation of genes involved in the ectopic lymphoid neogenesis process. This in turns leads to T and B cell recruitment, differentiation and activation, culminating in the organisation of ELS and localised germinal centres responses.*

Introduction

Ectopic lymphoid structures (ELS) are highly organised lymphoid aggregates that form in non-lymphoid tissue during chronic inflammation. These aggregates can harbour a functional germinal centre and have been detected in a wide range of tissues including in cancer, infection, organ transplantation and autoimmune diseases (1). ELS have a structure reminiscent of secondary lymphoid organs characterised by B and T cell segregation, high endothelial venules for leukocyte trafficking, follicular dendritic cell networks supporting affinity maturation and B cell survival, and subsequent local generation of auto-reactive plasma cells (2).

In Sjögren's syndrome (SS), a chronic autoimmune disease affecting the exocrine glands, lymphocytes can infiltrate the lacrimal and salivary glands (SGs) where they form ELS in a subset of patients (3). Here ELS function as niches for autoreactive B cells and can correlate with an advanced presentation of disease symptoms and systemic features (4, 5). Although the exact cause of SS is currently unknown, it has been hypothesised that viral infections may exacerbate or drive the disease. Pertinent to this, Epstein-Barr virus was recently highlighted as a driver of lymphocyte activation at ectopic germinal centres (6), and when taken together with the known interferon signature present in SS patients (7) this suggests that viral activation of ectopic lymphoid neogenesis (ELN) may be a key step in disease evolution.

The precise mechanisms that underpin ELN are not currently known despite the structural similarities in the organisation of ELS and SLOs. Lymphoid tissue inducer (LTi) and organiser (LTo)

cells are of particular importance in the initiation of secondary lymphoid organogenesis (8), however during ELN different cell types take over these roles and the process heavily relies on chemokines including lymphotoxins, CXCL13, CCL19 and CXCL12 (9-11). In SS, SG stromal cells including ductal epithelial and endothelial cells secrete CXCL13 and CCL21 among many others, attracting both innate and adaptive cells to the inflamed area (3). Neutrophils (12), macrophages (13) and dendritic cells (DCs) (14) can play important roles in the generation of ELS in different experimental settings. For example, neutrophil depletion in neonatal mice attenuated LPS-induced ELS formation in the lung via a decrease in APRIL (a proliferating ligand) and IL-21 (12), both mediators of B cell activation, proliferation and function. Similarly, elimination of DCs in the lung after influenza virus infection led to a reduction in ectopic germinal centre reactions and reduced numbers of class-switched plasma cells (14). Furthermore, in a mouse model of aortic ELN, macrophages were able to act in a similar way to LTi cells by expressing high levels of TNF-α and membrane-bound lymphotoxin-α (TNF-β) (13).

Once ELS begin to develop, follicular dendritic cells (stromal cells that facilitate B cell activation and antibody maturation) become the main source of CXCL13, recruiting adaptive immune cells to the area which subsequently play an active role in secreting further cytokines and chemokines (4). Recruited T and B cells organise into segregated areas thanks to gradients of CCL19 and CXCL13 and specialised T follicular helper (Tfh) cells are able to migrate to the B cell area due to the expression of CXCR5 (15). Here Tfh cells secrete IL-21, promoting B cell activity and maturation (16). Recently, we have also shown that Tfh cell-related genes and IL-21, key factors in T-B cell cross-talk in ELS are the most upregulated genes in ELS+ SS patients (17).

Several murine models of SG inflammation have previously been developed in an attempt to recapitulate one or multiple aspects of human SS. One of the predominating spontaneous models is the non-obese diabetic (NOD) mouse and its derivatives. As well as developing type 1 diabetes, the NOD mouse is also characterised by immune cell infiltration to the exocrine glands, reduced secretion of saliva and tears and SS-associated autoantibodies (18). Other genetic models of SS include the Phosphoinositide 3-kinase (*PI3K*) KO and the *Id3* KO which lead to impaired T cell proliferation and selection and lymphocytic infiltration into the exocrine glands with production of anti-Ro and anti-La antibodies (19-21). Other models focus on the B cell component of SS, for example the B cell activating factor (BAFF) transgenic mouse. This mouse, which over expresses BAFF, displays B cell infiltration to the salivary glands and loss of secretory function (22). Finally, inducible models utilise Ro, M3R or other antigens to immunise mice leading to autoantibody production and impaired SG function (23, 24).

Recently, we demonstrated that a virus-induced murine model of SG inflammation and ELS formation developed in our laboratory (25), can be used to study the role of key players in ELN (25-28). This model recapitulates some of the characteristics of SS, including periductal lymphoid aggregates, ELS and breach of self-tolerance within 19 days of viral infection (25). While the knowledge of ELN is growing rapidly, there are still many features of this process that when elucidated might not only inform on the biology of ELS but also on their role in disease pathology. In the present study we have utilised our viral inducible model of ELS development to phenotypically characterise the innate and adaptive immune cell infiltrate from onset of viral infection to fully formed ELS, with regards to the cellular and genetic components that that underpin ELN.

Methods

Mice and in vivo methods

Female C57BL/6 mice 10–13 week-old were used for this study. Animals were housed under standard conditions at the Biomedical Service Unit at Queen Mary University of London and provided food and water *ad libitum*. All procedures were performed with approval from the local Animal Ethics and Welfare Committee and under a Home Office project license (P29EDC088) according to Home Office regulations. Replication deficient adenovirus 5 (AdV5) was administered to the murine submandibular SG via retrograde cannulation as described previously (25). Briefly, mice were anesthetised then positioned to allow access to the secretory duct of the submandibular gland. A concentrated (at least 10^9 pfu/mL) stock of the replication deficient Adv5 solution was administered to the gland via a cannula positioned inside the gland. The mice were then returned to their cage for the duration of the experiment.

Flow cytometry

Mice were culled at 3, 5, 7, 10, 12, 19 or 26 days post cannulation (dpc) via CO_2 inhalation and subsequently the SGs excised and placed into DMEM + 2% FBS. Tissue was digested using 3.7 mg/mL Collagenase D. Dead cells were marked using Zombie Aqua Fixable Viability dye (Table I). Cells were then incubated with fluorescently conjugated antibodies (BioLegend). For intracellular staining, cells were fixed and permeabilised using the Foxp3/Transcription Factor Staining Buffer Set (eBioscience) prior to incubation with the appropriate antibody mix. Where appropriate, a dump channel was used to exclude non relevant populations and samples were run on an LSR Fortessa cytometer (BD Biosciences). A table of antibodies is presented in Table I and gating strategies are shown in the supplementary information.

Immunofluorescence

SGs were excised and placed into optimal cutting temperature medium (OCT) and frozen at -80 degrees. 6μm sections were fixed in ice-cold acetone and blocked with antibody diluent buffer (TBS containing 10% vol/vol horse serum, 1% w/vol bovine serum albumin). Directly conjugated CD11c (BioLegend 117311) or unconjugated F4/80 (Sertotec MCA497G) were incubated on the tissue for 1 hour. Secondary goat anti-rat (Invitrogen A21434) conjugated antibody was used to visualise the F4/80 and all sections were counter stained with DAPI.

Table I. Flow cytometry antibodies used.

Target	Fluorophore	Cat number	Clone	Dilution	Panel
Ly6C	Alx488	Biolegend 128022	HK1.4	1 in 1600	G/M
CD45	PerCp/Cy55	Biolegend 103131	30-F11	1 in 800	G/M, T, Tcyt, B
Siglec-H	APC	Biolegend 129611	551	1 in 200	G/M
CD3	APC/Cy7	Biolegend 100221	17A2	1 in 80	G/M, B
CD19	APC/Cy7	Biolegend 115529	6D5	1 in 100	G/M
NK 1.1	APC/Cy7	Biolegend 108724	PK136	1 in 167	G/M, T, T cyt, B
Siglec-F	BV421	Biolegend 155509	S17007L	1 in 100	G/M
CD11b	BV605	Biolegend 101257	M1/70	1 in 200	G/M
Ly6G	BV650	Biolegend 127641	1A8	1 in 100	G/M
CD64	BV711	Biolegend 139311	X54-5/7.1	1 in 20	G/M
MHCII	Pe/Dazzle	Biolegend 107648	M5/114.15.2	1 in 400	G/M
B220	APC-Cy7	Biolegend 103223	RA3-6B2	1 in 167	T, T cyt
Gr1	APC-Cy7	Biolegend 108423	RB6-8C5	1 in 500	T, T cyt, B
F480	APC-Cy7	Biolegend 123117	BM8	1 in 167	T, T cyt, B
PD-1	BV785	Biolegend 135225	29F.1A12	1 in 800	T cyt
CXCR5	BV650	Biolegend 145517	L138D7	1 in 50	T cyt, B
CD25	BV605	Biolegend 102035	PC61	1 in 167	T cyt
CD4	PE/Cy7	Biolegend 100421	GK1.5	1 in 400	T, T cyt
CD127	Pe-CF594	Biolegend 135031	A7R34	1 in 400	T cyt
IL17A	Alx488	Biolegend 506909	TC11-18H10.1	1 in 400	T cyt
IL-4	BV710	Biolegend 504133	11B11	1 in 100	T cyt
IFNγ	PE	Biolegend 505807	XMG1.2	1 in 800	T, T cyt
CD44	Alx488	Biolegend 103015	IM7	1 in 200	T
CD3	BV785	Biolegend 100355	145-2C11	1 in 167	T
CD8	BV650	Biolegend 100741	53-6.7	1 in 167	T
CD62L	BV605	Biolegend 104437	MEL-14	1 in 167	T
Granzyme B	Alx647	Biolegend 515405	GB11	1 in 80	T
GL7	FITC	BD 553666	GL7	1 in 133	B
CD1d	Alx647	Biolegend 123511	1B1	1 in 200	B
B220	BV785	Biolegend 103245	RA3-6B2	1 in 167	B
CD21	PE	Biolegend 123409	7E9	1 in 800	B
IL-10	BV421	Biolegend 505021	JES5-16E3	1 in 50	B

Adoptive transfer of monocytes

Monocytes were sorted from CD45.2 bone marrow cells using the Miltenyi negative selection monocyte isolation kit. 1x10^6 monocytes were adoptive-transferred via tail intravenous injection to CD45.1 recipients 1 day prior to AdV5 cannulation. SGs were removed and analysed by flow cytometry at 1, 3, 6, 10 and 18 dpc.

Gene expression analysis

CD11b+ cells were isolated by positive magnetic selection (EasySep) from murine SGs and RNA extracted using the Arcturus picopure RNA isolation kit (ThermoFisher). RNA was reverse transcribed using the Thermoscript IV reverse transcription kit and cDNA analysed with 48.48 Dynamic Array™ IFC for Gene Expression (Fluidigm).

Statistical analysis

Statistical analysis was performed using GraphPad Prism version 7. For multiple comparisons, differences in quantitative data were analysed using the non-parametric Kruskal-Wallis test with by Dunn's *post-hoc* correction. Correlation analysis was performed using spearman rank correlation analysis. A p value <0.05 was considered statistically significant. *p<0.05, **p<0.01, ***p<0.001, ****p<0.0001.

Results

Early infiltration of the salivary gland is characterised by organised innate cell influx dominated by myeloid-derived cells

Retrograde cannulation was previously validated as an effective method to specifically deliver a replication deficient AdV5 locally to the murine submandibular SG to induce the formation of ELS within SG (25). ELS formation is identified by the formation of T/B aggregates in discrete areas characterised by the differentiation of HEV in the T cell-rich area and FDCs within the B cell follicle (25). Here we examine the innate and adaptive response to the virus at early and later time points. Firstly, by focussing on the early time points we show that CD11b+ cells account for a large proportion of total CD45+ cells that infiltrate the gland within the first 5 days after cannulation. From 7 dpc, a second peak of CD45+ cells influx is accounted for by lymphocytic infiltration (Fig. 1a-b). Subset analysis of innate immune cells shows that eosinophils and neutrophils rapidly and transiently infiltrate the gland (Fig. 1a-b). Conversely macrophages, monocytes and DC infiltration remain at levels above unchallenged control SG for the duration of the experiment up to 19 dpc (Fig. 1a-b).

Inflammatory monocytes recruited to the salivary glands from the peripheral compartment rapidly differentiate into F4-80+ macrophages

To determine whether monocytes migrate to the SG and differentiate into inflammatory macrophages, donor CD45.2 Ly6C+ bone marrow monocytes were adoptively transferred to CD45.1 mice 1 day prior to cannulation and followed for 18 days using the macrophage markers MHC-II and F4-80 (29). CD45.2 donor monocytes quickly migrate from the periphery to the SG within 1 week of infection and steadily acquire the expression of MHC-II and F4/80 whilst completely losing Ly6C by 18 dpc (Fig. 1c). While inside the SG, DCs and macrophages are both intimately associated with the diffuse inflammatory response within 7 dpc. However, by 10 dpc DCs selectively localise within the focal aggregates of immune cell clusters whilst macrophages are excluded from the developing ectopic lymphoid follicle and consequently locate around the edges of the *foci* and in the surrounding tissue (Fig. 1d).

The large preponderance of the myeloid infiltrate within the first week of infection, prior to the recruitment of T and B cells, strongly suggested that innate immune cells that infiltrate the SG at early time points may orchestrate the subsequent development of ELS. We therefore sought to investigate the production of inflammatory mediators

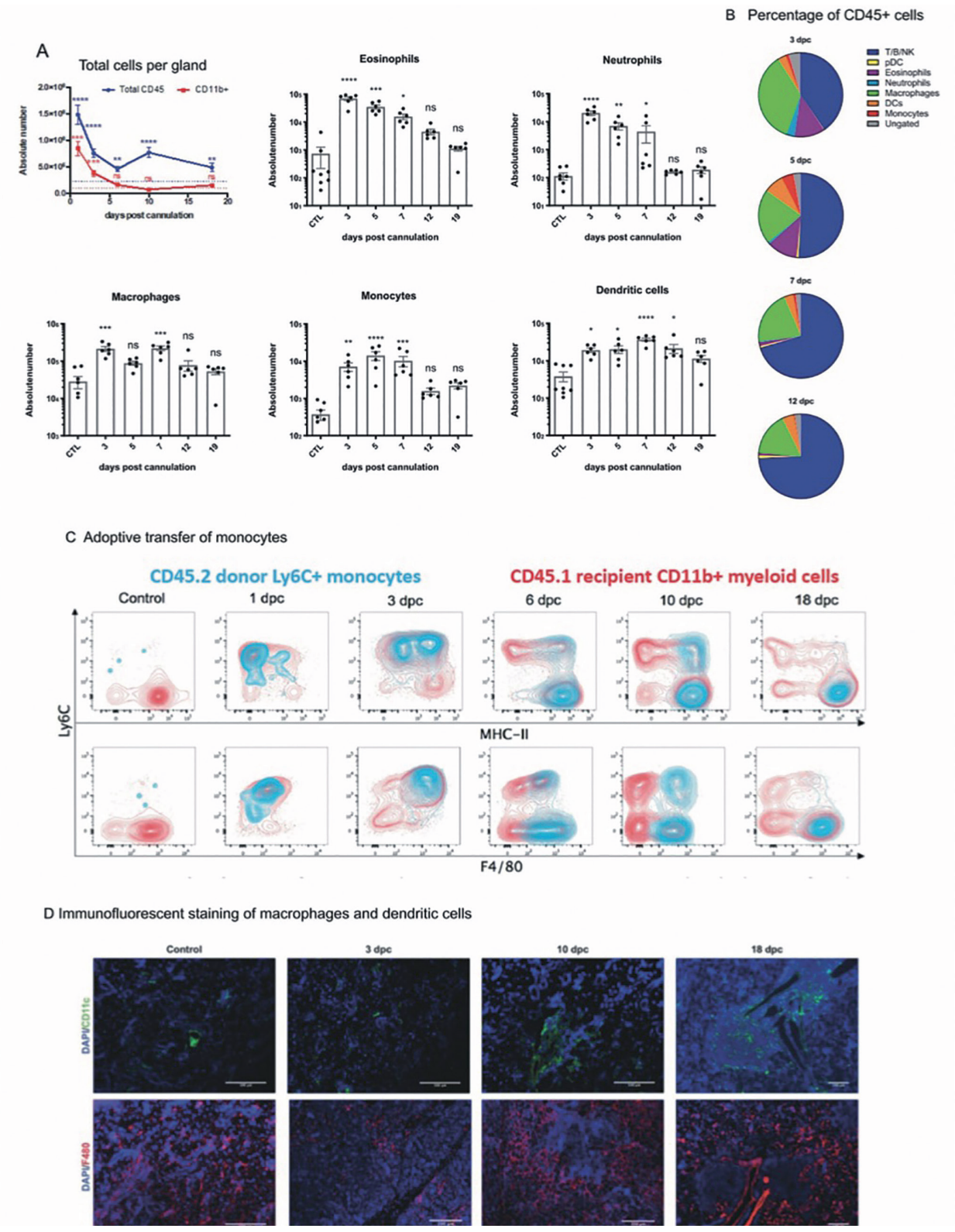

Fig. 1. Myeloid and granulocytes infiltrate the gland in the first week post cannulation.
A: Absolute number of total CD11b and CD45 cells per gland post cannulation and respective numbers of eosinophils, neutrophils, macrophages, monocytes and dendritic cells in the uncannulated control (n=8) and at 3 (n=6), 5 (n=6), 7 (n=6), 12 (n=6) and 19 (n=6) days post cannulation. **B:** Percentage of myeloid and granulocytes subsets of total viable CD45$^+$ cells in the uncannulated control (n=8) and at 3 (n=6), 5 (n=6), 7 (n=6) and 12 (n=6) days post cannulation. **C:** SG infiltrate in mice with adoptively transferred CD45.2 Ly6C+ monocytes to CD45.1 recipient mice 1 day prior to AdV cannulation shows gradual accumulation of macrophage features post infection. Data in A is represented by mean ± SEM and statistics are Kruskal-Wallis test with Dunns *post hoc* correction comparing each time point against the control. **D:** Immunofluorescent staining images of dendritic cells (CD11c+, green) and macrophages (F480+, red) in the mouse SG of uncannulated controls, 3, 10 and 18 days post cannulation.

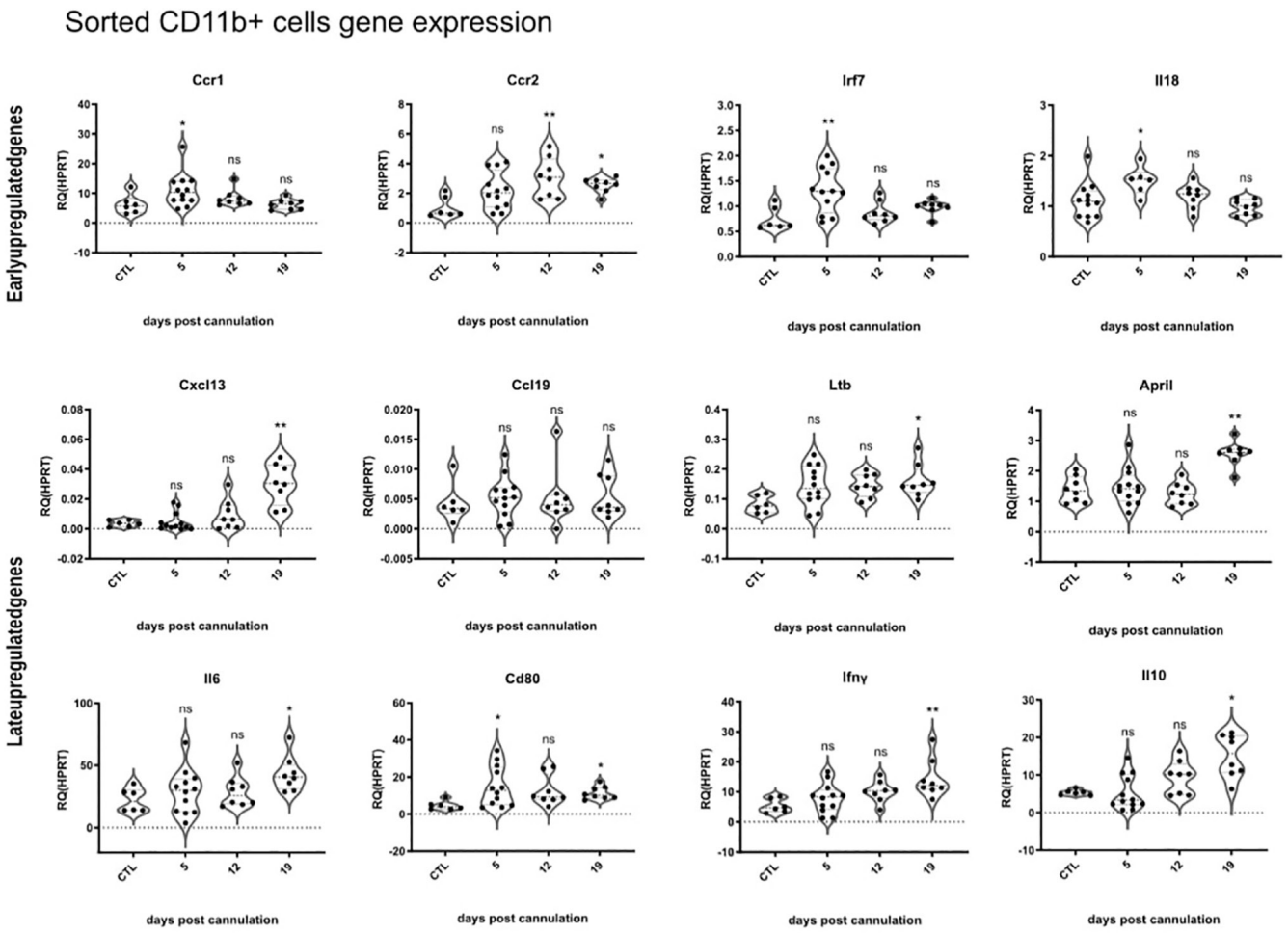

Fig. 2. Gene Expression of myeloid compartment.
RT-PCR on sorted CD11b+ cells in the uncannulated control (n=6), 5 (n=12), 12 (n=8) and 19 (n=8) days post cannulation.
Data is represented by mean ± SEM. Statistics are Kruskal-Wallis test with Dunns *post-hoc* correction comparing each time point against the control.

and lymphoid chemokines at transcriptomic level by myeloid cells at different time points after viral infection.

Activated CD11b+ myeloid cells in the gland express key lymphocyte cytokines, chemoattractants and lymphoid chemokines

In the early phases of ELS formation (5-12 dpc), SG CD11b+ myeloid cells express high levels of *Ccr1*, *Ccr2*, *Irf7*, *Il18* and *Cd80* genes (Fig. 2). *Ccr1* and *Ccr2*, receptors for the chemokines RANTES (Regulated on Activation, Normal T Expressed and Secreted) and CCL2 (monocyte chemoattractant protein-1) respectively, are thus likely responsible for aiding the migration of myeloid cells into the inflamed SG tissue. *Irf7* (interferon regulatory factor 7), part of the type-I interferon (IFN-I)-inducible genes involved in host response to viral infections, *Il18* which promotes T cell differentiation into Th1 cells and *Cd80* which aids in B-T cell co-stimulation, are all involved in the lymphocytic response to viral infections, as expected at the early time points.

Of relevance, at later time points (by 12-19 dpc), myeloid cells upregulate key mediators involved in B cell recruitment, survival, proliferation and activation including *Cxcl13 (*but not *Ccl19)* and *April* as well as the proinflammatory cytokines *Il6* and *Ifng*. Interestingly myeloid cells also upregulate *Ltb* at 19dpc, a key molecule of the TNF family involved in lymphoid tissue formation and *de novo* expression of lymphoid chemokines (Fig. 2). Finally, we observed that myeloid cells significantly upregulate *Il10* gene compared to controls by 19 dpc. IL-10, an anti-inflammatory cytokine, may be important in the resolution of the immune response in the SG and the regression of ELS over an even longer time course.

Functional phenotype of infiltrating T cells

Next, we characterised $CD4^+$ and $CD8^+$ T cells that infiltrate the SG post cannulation with respect to their memory phenotype and effector functions. $CD4^+$ and $CD8^+$ T cells remain in low numbers at 5 dpc but then begin to infiltrate the submandibular SG by 12 dpc and remain in high numbers throughout the duration of the experiment (Fig. 3a) as also previously described (26). To determine the functional phenotype of these cells we performed an analysis of the central memory ($CD44^+$ $CD62L^+$) and effector memory ($CD44^+$ CD62L-) (30) cell populations in the SGs. Compared to the steady state, there is an expansion of central memory $CD4^+$ and $CD8^+$ T cells immediately after cannulation which

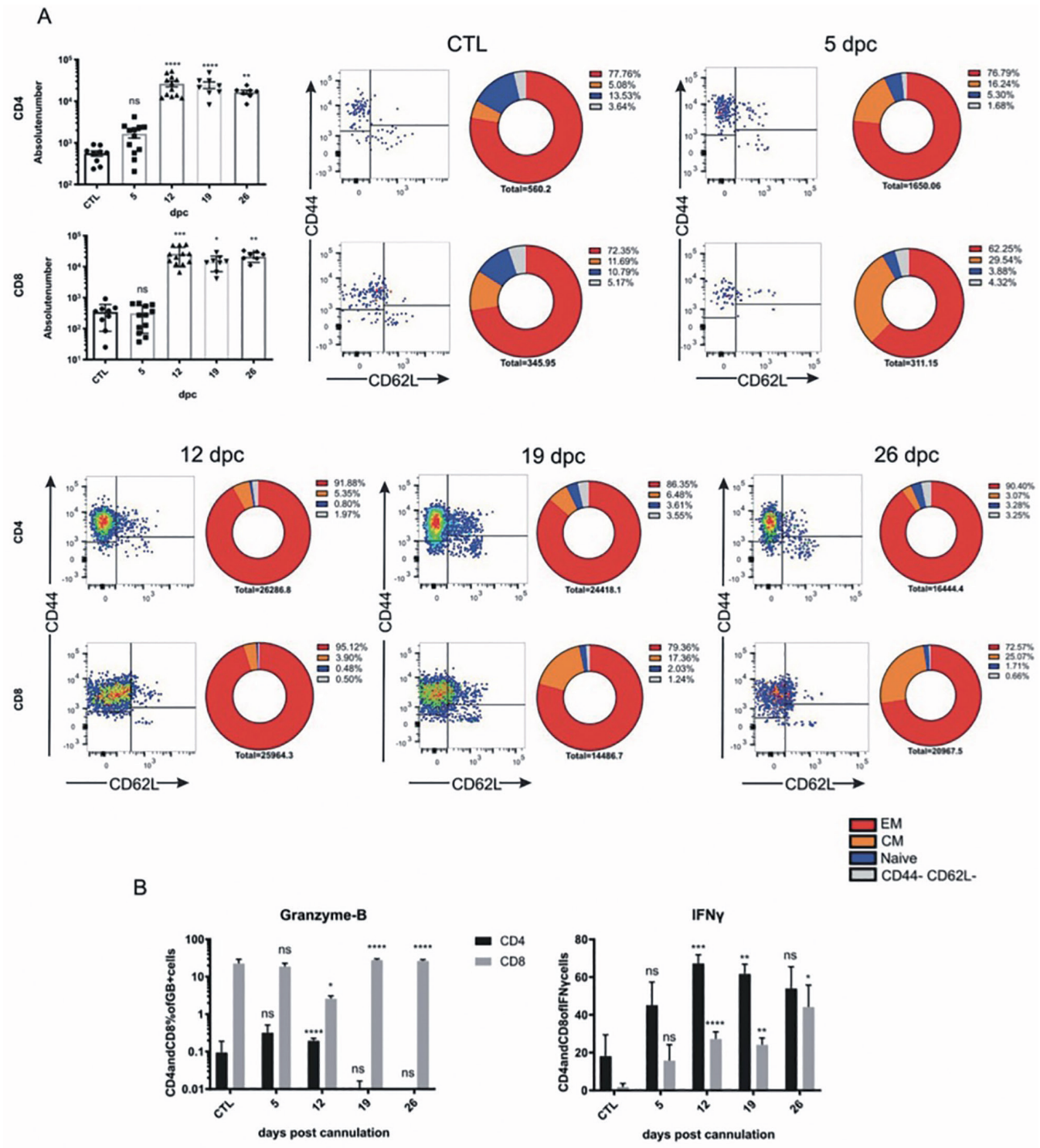

Fig. 3. CD4⁺ and CD8⁺ T cells infiltrate the salivary gland by 12 dpc and begin to produce granzyme B and IFNγ.
A: CD4+ and CD8+ effector memory (CD44+ CD62L-) T cells and central memory (CD44+ CD62L+) T cells representative plots from salivary gland and quantification of the proportions of naïve, Tcm and Tem cells out of the total CD4 or CD8 population respectively in the uncannulated control (n=9) and at 5 (n=12), 12 (n-12), 19 (n=8) and 26 (n=7) days post cannulation. **B**: T cell effector functions including granzyme-B and IFNγ production in the CD4+ or CD8+ T cell compartment in the uncannulated control (n=9) and at 5 (n=12), 12 (n-12), 19 (n=8) and 26 (n=7) days post cannulation.
Data is represented by mean ± SEM. Statistics are Kruskal-Wallis test with Dunns *post-hoc* correction comparing each time point against the control.
Tcm: T central memory; Tem: T effector memory.

decreases in proportion by 12 dpc. Effector memory cells are the dominant phenotype in both CD4 and CD8 T cell subsets and expand further during the second and third week post cannulation, whereas naïve cells disappear almost completely. By 19 dpc, the CD8⁺ T cell central memory phenotype expands and remains high throughout the duration of the experiment, whilst in the CD4⁺ subset the effector memory cells remain the most prevalent type. Focussing on the

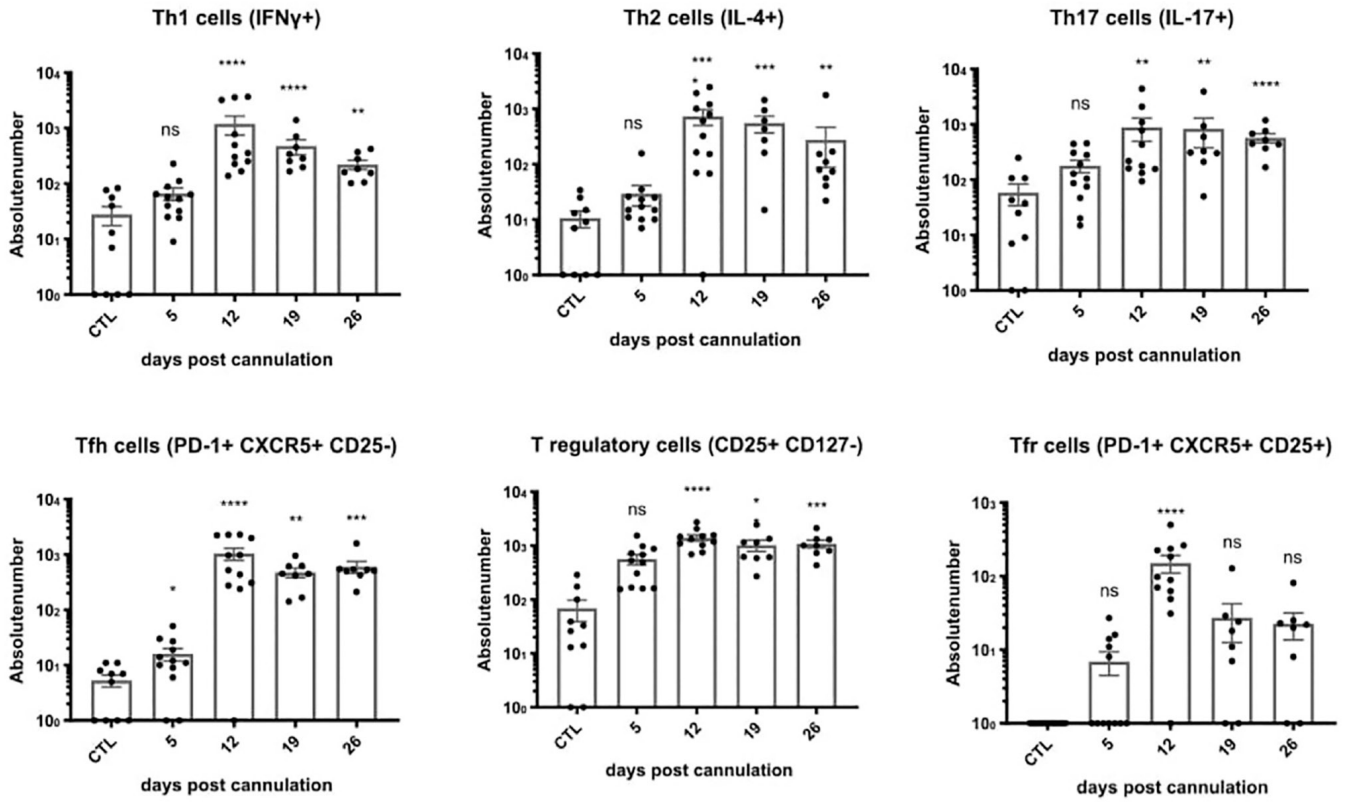

Fig. 4. T helper subsets infiltrate the gland at 12 dpc.
Absolute cell numbers in total SG of Th1 (IFNγ+) cells, Th2 (IL-4+) cells, Th17 (IL-17+) cells, Tfh (PD-1+, CXCR5+, CD25-) cells, T regulatory (CD25+ CD127-) cells and Tfr (PD-1+ CXCR5+ CD25+) cells. All populations gated on total CD4+ cells and shown in the uncannulated control (n=10) and at 5 (n=12), 12 (n=12), 19 (n=8) and 26 (n=8) days post cannulation. Data is represented by mean ± SEM. Statistics are Kruskal-Wallis test with Dunns *post-hoc* correction comparing each time point against the control.

T cell effector functions, granzyme-B is produced by both $CD4^+$ and $CD8^+$ T cells by 12 dpc after which point $CD8^+$ cells become the main cytotoxic T cells (Fig. 3b). IFN-γ producing T cells quickly expand in number after infection with AdV5 in both the $CD4^+$ and $CD8^+$ compartment (Fig. 3b). Here, $CD4^+$ T cells are high producers of this cytokine throughout the time course. Importantly and shown previously, NK cells are also key producers of granzyme-B and IFN-γ within the SG at early time points after viral infection (between 3 and 10 dpc) (27). We therefore hypothesise that while NK cells greatly decrease in number by 10 dpc (27), T cells expand and take over the production of these effector molecules.

$CD4^+$ T cells largely infiltrate the salivary gland by 12 dpc, differentiate into subsets closely involved in ELS formation, and precede germinal centre B cell differentiation

Focussing on $CD4^+$ lymphocytic subset allows us to characterise and dissect the type of immune response taking place in the murine SG around the time of ELN development (day 12pc onwards). Th1, Th2, T regulatory and Th17 cells all increase in number although not significantly by 5 dpc and are all present in significantly higher numbers than in the control glands by 12 dpc (Fig. 4). Interestingly, we can also detect a large influx of $CXCR5^+PD1^+CD25^-$ Tfh cells by 12 dpc in parallel with the concomitant differentiation of $CXCR5^+PD1^+CD25^+$ Tfr cells (Fig. 4). $B220^+$ B cells in general and follicular B cells in particular, do not infiltrate the SG until 12 dpc but are highly increased compared to the level detected in control glands at all late time points (Fig. 5a). Germinal centre ($GL7^+$) B cells were not apparent until 19 dpc, indicating that fully formed germinal centres do not take place until at least 19 dpc. In keeping with the known role of Tfh cells in the regulation of germinal centre responses, by 12 dpc Tfh cells and GC B cell numbers closely and positively correlate in the SG (Fig. 5b).

Discussion

ELS are a common (30-40% of patients) feature of SS and are present in many other autoimmune diseases where they correlate with worse disease progression and increased risk of developing complications (4, 31, 32). Here, we report for the first time a detailed longitudinal analysis of the overall shape and timeline of the leukocytic infiltrate in an AdV5-mediated inducible murine model of sialadenitis that recapitulates many features of ELS formation including T/B cell segregation, FDC networks and fully functional AID+ germinal centres (25). In particular we show that following AdV5 infection, a stepwise infiltration of myeloid and other innate immune cells dominate the early SG immune response after viral infection during the first week, whereby inflammatory monocytes are recruited from the periphery and rapidly mature into

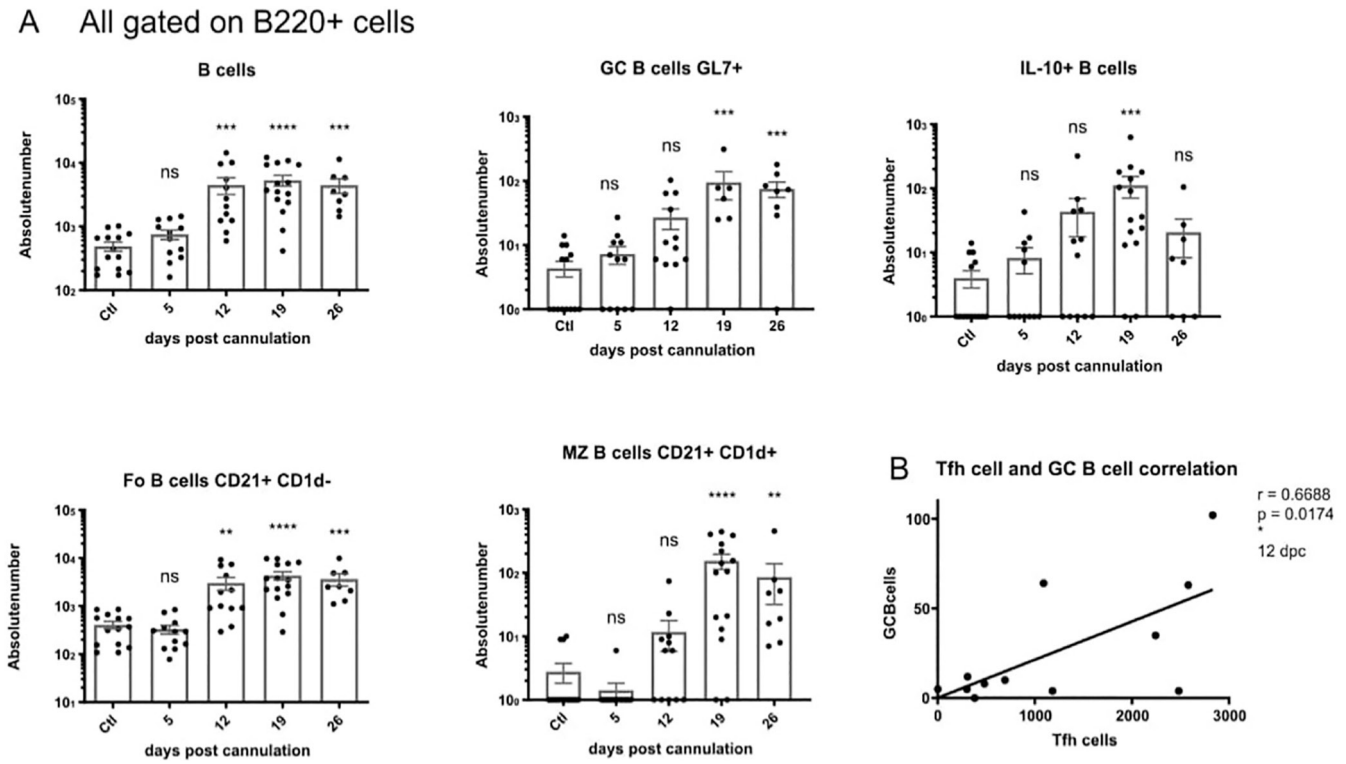

Fig. 5. B cell subset infiltration follows T cells and arrange into ELS in the gland.
A: B cells, germinal centre B cells (GL7+), IL-10+ B cells, follicular B cells (CD21+ CD1d-) and marginal zone B cells (CD21+ CD1d+) absolute counts in the whole salivary gland. All populations gated on total B220+ B cells and shown in the uncannulated control (n=14), and at 5 (n=12), 12 (n=12), 19 (n=15) and 26 (n=8) days post cannulation. Data is represented by mean ± SEM. Statistics are Kruskal-Wallis test with Dunns *post hoc* correction comparing each time point against the control.
B: Correlation between Tfh cells and germinal centre B cell frequency at 12dpc in the salivary gland. Correlation based on Spearman rank correlation analysis.

macrophages. Upon analysis of the gene expression profile of CD11b+ sorted myeloid cells, we were able to determine that myeloid cells upregulate *Ccr1*, a receptor that binds to RANTES commonly released by virally infected epithelial cells, and *Ccr2* which aids in monocyte recruitment (33). Eosinophils and neutrophils are also recruited to the SG in the very early days following AdV5 infection however it is unclear whether these cells play a role in viral control, ELS formation or recruitment of lymphocytes to the gland. The only role that we can speculate here is that eosinophils are able to secrete Th2 polarising cytokines (34) that may explain the influx of IL-4+ T cells seen in our model.

An important finding of this work was that while CD11c+ DCs are found within lymphoid aggregates, macrophages are excluded from periductal *foci* and instead remain scattered throughout the gland. Given that this has also been detected previously in murine inflammatory arthritis models (35), it highlights that whereas macrophages are involved in the general inflammatory response, including the recruitment of additional immune cells into the gland, DCs play a more prominent role in the organisation and maintenance of the developing lymphoid aggregates. This is likely related to both direct T cell activation as well as the secretion of lymphoid chemokines. This is also corroborated by our recent evidence of DC-LAMP+ activated DCs within T cell areas of ELS in SS SG (26) which may indicate an important cross-talk between these two cell subsets.

The work presented here further complete the elucidation of the local immune response leading to ELS formation in the SG after viral infection. While we previously showed that in our inducible model of sialoadenitis NK cells, albeit important for early viral control, were redundant for ELS formation (27), in collaboration with Barone *et al*. we reported a key role for stromal and epithelial cells in secreting CXCL13 and CXCL12, respectively, in response to rapid secretion of IL-22 following AdV infection (28). Here, we further demonstrate that by 12dpc also CD11b+ myeloid cells are an abundant source of *Cxcl13* and *April*, in parallel with the abundant B cell infiltration observed from 12dpc. Conversely, given that B cell infiltration is not observed at the time of CXCL13 production by stromal cells in response to IL-22, our data suggests that DC-derived CXCL13 is critical for ELS formation in our model, similarly to previous evidence in ELN in the murine lungs induced by influenza virus. Additionally, we showed that activated CD11b+ myeloid cells produce increased levels of *Il18, Irf7* and *Cd80* by 5 dpc as well as *Il6* and *Ifng* by 19 dpc, thus contributing to sustain the local immune response throughout the process of ELS formation. These findings are also supported by previous work showing CXCL13 production by macrophages and recently extravased monocytes within lymphoid aggregates of rheumatoid arthritis patients (36). Moreover, increased IL-18 was

previously described in the SG of SS patients where this cytokine may amplify the production of other proinflammatory cytokines including IL-6, IL-8 and IL-17 and drive Th1 differentation (37). Taken together, our results as well as previously published work highlight that a multitude of early responding cell types are together responsible for driving lymphocytic infiltration and lymphoid organisation within the SG.

Once they infiltrate the virally-infected SG, $CD4^+$ T cells show a predominately IFN-γ+ effector phenotype, although also infiltrating Th2 and Th17 cells could be detected after viral infection, whereas the main role of $CD8^+$ T cells seems to be in the release of the serine protease granzyme-B displaying a mixed effector and central memory phenotype. With regards to later time points closely associated with ELS formation, as expected we reported a large infiltration in CXCR5+ Tfh cells, recently implicated in ELS formation and MALT-lymphoma development in patients with SS (17), which were positively correlated with the differentiation of GL7+ germinal centre B cells. Thus, although here we do not provide direct functional evidence, Tfh cells likely play a key role in the activation of B cells recently migrated into the gland leading to an ectopic GC response during the third week post-infection. These data are in keeping with our previous evidence of AID+ functional ectopic GC responses in our model, associated with the onset of circulating anti-AdV as well as autoantibodies (25), similarly to what has been observed in SS patients with ELS in their SGs (5). Another finding of note was the evidence that Tfr cells infiltration was observed, albeit only transiently, in the murine SG post infection. Tfr cells are crucial in the control of physiological germinal centre responses (38) and their potential role in regulating autoimmunity in SS has only recently been investigated (39). Similarly, we also reported a transient increase in IL-10 secreting B cells in our model. These cells have previously been reported in SS and in murine SS models where they negatively correlate with Tfh cells (40).

The present study provides a detailed description of the kinetics of immune cell infiltration leading to the ELS formation in an AdV5-mediated inducible murine model of sialadenitis. A more functional approach (with blockade/depletion experiments) would provide support to the hypothesised stepwise role of DCs, monocyte and macrophage activation in ELS formation and maintenance. At present, we were not able to discriminate the role of each specific population in our model, representing the main limitation of the study. Additionally, because myeloid-derived cytokines such as IL-18/IL-12 have been differentially associated with increased risk of lymphomagenesis (41), it would have been of interest to provide further support of the mechanisms leading to lymphroliferation. However, due to the non-replicative nature of the viral vector used to trigger the SG inflammation, a spontaneous resolution of the inflammation usually occurs from week 4/5 onward, making this model unsuitable to mimic chronic inflammation and lymphoproliferative disorders within the salivary glands.

Overall, our model is highly suitable to clarify and manipulate pro- *versus* anti-inflammatory immune responses taking place in the SG to modulate ELS formation and function.

References

1. PITZALIS C, JONES GW, BOMBARDIERI M, JONES SA: Ectopic lymphoid-like structures in infection, cancer and autoimmunity. *Nat Rev Immunol* 2014; 14: 447-62.
2. JONES GW, JONES SA: Ectopic lymphoid follicles: inducible centres for generating antigen-specific immune responses within tissues. *Immunology* 2016; 147: 141-51.
3. BARONE F, BOMBARDIERI M, MANZO A *et al*.: Association of CXCL13 and CCL21 expression with the progressive organization of lymphoid-like structures in Sjögren's syndrome. *Arthritis Rheum* 2005; 52: 1773-84.
4. BOMBARDIERI M, LEWIS M, PITZALIS C: Ectopic lymphoid neogenesis in rheumatic autoimmune diseases. *Nat Rev Rheumatol* 2017; 13: 141-54.
5. JONSSON M V, SKARSTEIN K, JONSSON R, BRUN JG: Serological implications of germinal center-like structures in primary Sjögren's syndrome. *J Rheumatol* 2007; 34: 2044-9.
6. BARCELOS F, MARTINS C, MONTEIRO R *et al*.: Association between EBV serological patterns and lymphocytic profile of SjS patients support a virally triggered autoimmune epithelitis. *Sci Rep* 2021; 11: 1-12.
7. MARIETTE X, GOTTENBERG J-E: Pathogenesis of Sjögren's syndrome and therapeutic consequences. *Curr Opin Rheumatol* 2010; 22: 471-7.
8. VAN DE PAVERT SA, MEBIUS RE: New insights into the development of lymphoid tissues. *Nat Rev Immunol* 2010; 10: 664-74.
9. TANG H, ZHU M, QIAO J, FU Y-X: Lymphotoxin signalling in tertiary lymphoid structures and immunotherapy. *Cell Mol Immunol* 2017; 14: 809-18.
10. CORSIERO E, BOMBARDIERI M, MANZO A, BUGATTI S, UGUCCIONI M, PITZALIS C: Role of lymphoid chemokines in the development of functional ectopic lymphoid structures in rheumatic autoimmune diseases. *Immunol Lett* 2012; 145: 62-7.
11. NAYAR S, CAMPOS J, SMITH CG *et al*.: Immunofibroblasts are pivotal drivers of tertiary lymphoid structure formation and local pathology. *Proc Natl Acad Sci USA* 2019; 116: 13490-7.
12. FOO SY, ZHANG V, LALWANI A *et al*.: Regulatory T cells prevent inducible BALT formation by dampening neutrophilic inflammation. *J Immunol* 2015; 194: 4567-76.
13. GUEDJ K, KHALLOU-LASCHET J, CLEMENT M *et al*.: M1 macrophages act as LTβR-independent lymphoid tissue inducer cells during atherosclerosis-related lymphoid neogenesis. *Cardiovasc Res* 2014; 101: 434-43.
14. GEURTSVANKESSEL CH, WILLART MAM, BERGEN IM *et al*.: Dendritic cells are crucial for maintenance of tertiary lymphoid structures in the lung of influenza virus–infected mice. *J Exp Med* 2009; 206: 2339-49.
15. CROTTY S: T follicular helper cell differentiation, function, and roles in disease. *Immunity* 2014; 41: 529-42.
16. KING C, TANGYE SG, MACKAY CR: T follicular helper (T_{FH}) cells in normal and dysregulated immune responses. *Annu Rev Immunol* 2008; 26: 741-66.
17. PONTARINI E, MURRAY-BROWN WJ, CROIA C *et al*.: Unique expansion of IL-21+ Tfh and Tph cells under control of ICOS identifies Sjögren's syndrome with ectopic germinal centres and MALT lymphoma. *Ann Rheum Dis* 2020; 79: 1588-99.
18. CHA S, NAGASHIMA H, BROWN VB, PECK AB, HUMPHREYS-BEHER MG: Two NOD idd-associated intervals contribute synergistically to the development of autoimmune exocrinopathy (Sjögren's syndrome) on a healthy murine background. *Arthritis Rheum* 2002; 46: 1390-8.
19. GUO Z, LI H, HAN M, XU T, WU X, ZHUANG Y: Modeling Sjögren's syndrome with Id3 conditional knockout mice. *Immunol Lett* 2011; 135: 34-42.
20. HAYAKAWA I, TEDDER TF, ZHUANG Y: B-lymphocyte depletion ameliorates Sjögren's syndrome in Id3 knockout mice. *Immunology* 2007; 122: 73-9.
21. OAK JS, DEANE JA, KHARAS MG *et al*.: Sjögren's syndrome-like disease in mice with T cells lacking class 1A phosphoinositide-3-kinase. *Proc Natl Acad Sci USA* 2006; 103: 16882-7.
22. GROOM J, KALLED SL, CUTLER AH *et al*.: Association of BAFF/BLyS overexpression and altered B cell differentiation with Sjögren's

syndrome. *J Clin Invest* 2002; 109: 59-68.
23. SCOFIELD RH, ASFA S, OBESO D, JONSSON R, KURIEN BT: Immunization with short peptides from the 60-kDa Ro antigen recapitulates the serological and pathological findings as well as the salivary gland dysfunction of Sjogren's syndrome. *J Immunol* 2005; 175: 8409-14.
24. IIZUKA M, WAKAMATSU E, TSUBOI H *et al*.: Pathogenic role of immune response to M3 muscarinic acetylcholine receptor in Sjögren's syndrome-like sialoadenitis. *J Autoimmun* 2010; 35: 383-9.
25. BOMBARDIERI M, BARONE F, LUCCHESI D *et al*.: Inducible tertiary lymphoid structures, autoimmunity, and exocrine dysfunction in a novel model of salivary gland inflammation in C57BL/6 mice. *J Immunol* 2012; 189: 3767-76.
26. LUCCHESI D, COLEBY R, PONTARINI E *et al*.: Impaired interleukin-27–mediated control of CD 4^+ T cell function impact on ectopic lymphoid structure formation in patients with Sjögren's syndrome. *Arthritis Rheumatol* 2020; 72: 1559-70.
27. PONTARINI E, LUCCHESI D, FOSSATI-JIMACK L *et al*.: NK cell recruitment in salivary glands provides early viral control but is dispensable for tertiary lymphoid structure formation. *J Leukoc Biol* 2019; 105: 589-602.
28. BARONE F, NAYAR S, CAMPOS J *et al*.: IL-22 regulates lymphoid chemokine production and assembly of tertiary lymphoid organs. *Proc Natl Acad Sci* 2015; 112: 11024-9.
29. CRANE MJ, DALEY JM, VAN HOUTTE O, BRANCATO SK, HENRY WL, ALBINA JE: The monocyte to macrophage transition in the murine sterile wound. *PLoS One* 2014; 9: e86660.
30. MAHNKE YD, BRODIE TM, SALLUSTO F, ROEDERER M, LUGLI E: The who's who of T-cell differentiation: human memory T-cell subsets. *Eur J Immunol* 2013; 43: 2797-809.
31. RISSELADA AP, LOOIJE MF, KRUIZE AA, BIJLSMA JWJ, VAN ROON JAG: The role of ectopic germinal centers in the immunopathology of primary Sjögren's syndrome: a systematic review. *Semin Arthritis Rheum* 2013; 42: 368-76.
32. CARUBBI F, ALUNNO A, CIPRIANI P *et al*.: A retrospective, multicenter study evaluating the prognostic value of minor salivary gland histology in a large cohort of patients with primary Sjögren's syndrome. *Lupus* 2015; 24: 315-20.
33. LI L, JIANG B-E: Serum and synovial fluid chemokine ligand 2/monocyte chemoattractant protein 1 concentrations correlates with symptomatic severity in patients with knee osteoarthritis. *Ann Clin Biochem* 2015; 52: 276-82.
34. ODEMUYIWA SO, GHAHARY A, LI Y *et al*.: Cutting edge: human eosinophils regulate T cell subset selection through indoleamine 2,3-dioxygenase. *J Immunol* 2004; 173: 5909-13.
35. JONES GW, BOMBARDIERI M, GREENHILL CJ *et al*.: Interleukin-27 inhibits ectopic lymphoid-like structure development in early inflammatory arthritis. *J Exp Med* 2015; 212: 1793-802.
36. CARLSEN HS, BAEKKEVOLD ES, MORTON HC, HARALDSEN G, BRANDTZAEG P: Monocyte-like and mature macrophages produce CXCL13 (B cell-attracting chemokine 1) in inflammatory lesions with lymphoid neogenesis. *Blood* 2004; 104: 3021-7.
37. SAKAI A, SUGAWARA Y, KUROISHI T, SASANO T, SUGAWARA S: Identification of IL-18 and Th17 cells in salivary glands of patients with Sjögren's syndrome, and amplification of IL-17-mediated secretion of inflammatory cytokines from salivary gland cells by IL-18. *J Immunol* 2008; 181: 2898-906.
38. LINTERMAN MA, PIERSON W, LEE SK *et al*.: Foxp3+ follicular regulatory T cells control the germinal center response. *Nat Med* 2011; 17: 975-82.
39. FONSECA VR, ROMÃO VC, AGUA-DOCE A *et al*.: The ratio of blood T follicular regulatory cells to t follicular helper cells marks ectopic lymphoid structure formation while activated follicular helper T cells indicate disease activity in primary Sjögren's syndrome. *Arthritis Rheumatol* 2018; 70: 774-84.
40. LIN X, WANG X, XIAO F *et al*.: IL-10-producing regulatory B cells restrain the T follicular helper cell response in primary Sjögren's syndrome. *Cell Mol Immunol* 2019; 16: 921-31.
41. MANOUSSAKIS MN, BOIU S, KORKOLOPOULOU P *et al*.: Rates of infiltration by macrophages and dendritic cells and expression of interleukin-18 and interleukin-12 in the chronic inflammatory lesions of Sjögren's syndrome: correlation with certain features of immune hyperactivity and factors associated with high risk of lymphoma development. *Arthritis Rheum* 2007; 56: 3977-88.